



An approach to optimize the production of solar desalination unit using the SMCEC principle

K. Zhani^a, H. Ben Bacha^{b*}

^aLaboratoire des Systèmes Electro-Mécaniques (LASEM), National Engineering School of Sfax, Sfax University, Tunisia

^bCollege of Engineering in Alkharj, King Saud University, BP 655-11946, Kingdom of Saudi Arabia

Tel. +966 (50) 6678408; email: hbacha@Ksu.edu.sa

Received 29 April 2009; accepted 1 October 2009

ABSTRACT

This paper tackles an optimization approach in order to boost the fresh water production of the SMCEC (Solar Multiple Condensation Evaporation Cycle) unit which is located at Sfax's engineering national school in Tunisia. This optimization approach is based upon the above mentioned design's improvement through adding into it a flat plate solar air collector and a humidifier. Then, the humidification dehumidification (HD) developed process is essentially composed of five components: a flat plate solar air collector, a flat plate solar water collector, a humidifier, an evaporation tower and a condensation tower. A global mathematical model based on heat and mass transfers is developed to investigate both the effect of different operating modes and that of the variation of functioning parameters and weather conditions on the fresh water production. The fresh water production of the most effective operating mode is compared to the SMCEC unit and as a result, it transpires that the fresh water production of the most effective operating mode has increased with comparison to the SMCEC production.

Keywords: Solar energy; Water desalination; Humidification-dehumidification; Operating modes; Mathematical model and optimization

1. Introduction

The availability of safe drinking water is becoming an increasingly important issue. Expanding populations, enhanced living standards and decreased availability of fresh water has catalyzed much research in the area of obtaining potable water. Since a large majority of the earth's water supply is salt water, desalination methods such as reverse osmosis and electrodialysis have been developed. In addition to the practical limitation of small-scale usage, these methods are energy demanding, costly for small amounts of

fresh water, require high maintenance due to the practical difficulties associated with the high operating temperature, like corrosion and scale formation and are generally coupled to fossil-fuel sources which have a negative impact on the environment. A potentially feasible alternative is solar powered desalination with a humidification-dehumidification principle. Solar energy is free, abundant and an environmentally friendly energy source. Combining the principle of Humidification-Dehumidification (HD) with solar desalination leads to an increase on the overall efficiency of the desalination system and therefore appears to be the best method of water desalination with solar energy [1].

*Corresponding author

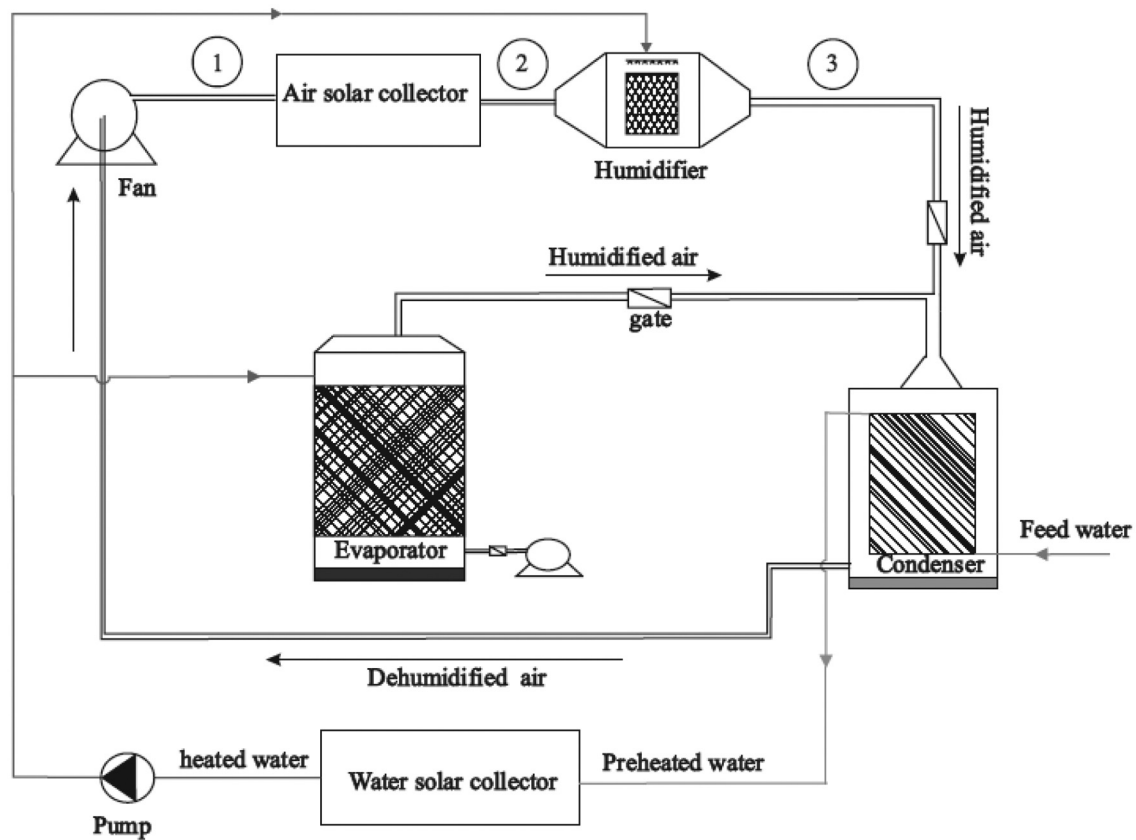


Fig. 1. Schematic diagram of the solar desalination system.

A review of the vast literature available on solar desalination has revealed many observations about the design, performance and the limitation of fresh water production of solar desalination units based on humidification dehumidification principle especially the SMCEC (Solar Multiple Condensation Evaporation Cycle) unit. The SMCEC unit is a new generation of water desalination installation by solar energy which is studied in 1999 by Ben Bacha et al. [2]. The SMCEC based desalination unit consists of three main parts: water solar collector, condensation tower and evaporation tower. Based upon the fact that the vapour carrying capability of air increases with temperature: 1 kg of dry air can carry 0.5 kg of vapour and about 670 kcal when its temperature increases from 30 °C to 80 °C [3], our approach to elevate the fresh water production of the SMCEC unit consists in increasing the capacity of air to load water vapor by heating and subsequent humidification of air at the exit of the condensation tower instead of rejecting or recycling it. So, to attend our objective it is necessary to integrate into the SMCEC unit a flat plate solar air

collector for heating air and a humidifier for its humidification. Then, the newly designed system is essentially composed of a flat plate solar air collector, a flat plate solar water collector, a humidifier, and a separate evaporator and condenser.

The main objectives of the work at hand are:

- To optimize the functioning of the solar desalination unit by developing three operating modes
- To investigate not only the effect of operating modes but also that of functioning and weather parameters on the fresh water production
- To compare the obtained results with Ben Bacha and Nafey's.

2. System description and thermodynamic behavior

The solar desalination system, object of this work, comprises air and water solar collector, humidifier and a separate evaporator and a condenser as it is shown in Fig. 1. Sea or brackish water which is preheated in the

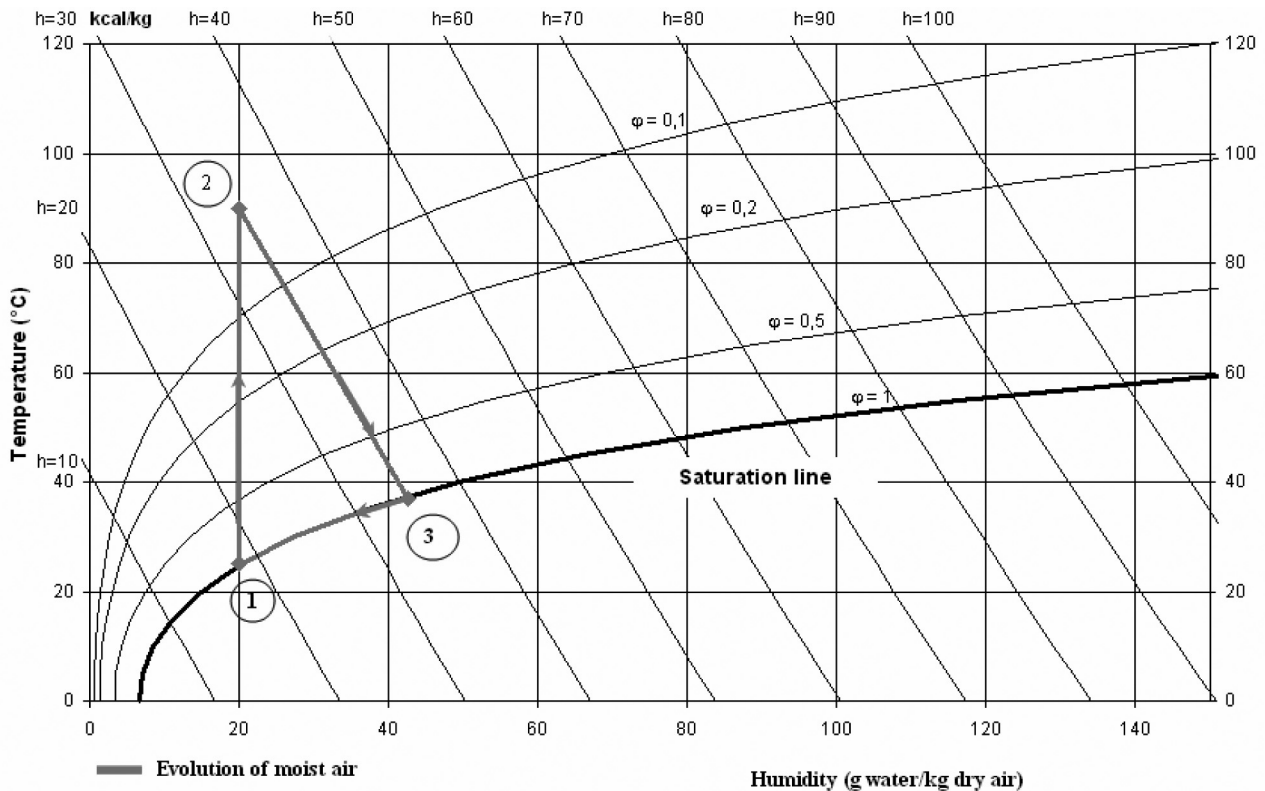


Fig. 2. Thermodynamic behavior of air through the HD process.

condensation tower, by the latent heat of condensation, and heated in the water solar collectors is pulverized into the humidifier and the evaporation tower. Due to heat and mass transfers between the hot water and the heated air stream in the humidifier in case of working in closed air loop and between the hot water and the ambient air stream in the evaporation tower in case of working in open air loop, the latter is loaded with moisture. To increase the surface of contact between air and water, and therefore to rise the rate of air humidification, packed bed is implanted in the tower of evaporation and the humidifier. The saturated moist air is then transported toward the tower of condensation where it enters in contact with a surface which its temperature is lower than the dew point of the air. The condensed water was collected from the bottom of the condensation tower, while the brine (the salty water exiting the evaporator and the humidifier) at the bottom of both the humidifier and evaporation tower will be either recycled and combined with the feed solution at the entry point or rejected in case of an increase of saltiness rates.

The utility of integrating into the SMCEC unit an air solar collector for heating air and a humidifier for a subsequent humidification can be explained by using

the psychrometric chart of moist air, also called h - x diagram [4,5], shown in Fig. 2. The humid air behavior is described using the psychrometric chart under the following assumptions:

- The humid air exiting the condensation tower is supposed saturated.
- The temperature of humid air at the outlet of air solar collector is about 90 °C.
- The process of humidification is adiabatic.
- The dehumidification process lies on the saturation line.

As shown in Fig. 2, the idea of heating air after its dehumidification in the condensation tower (point 1) instead of rejecting it, diminishes its relative humidity under 0.1 (point 2) which in its turn leads to increasing the capacity of air to load water vapor. The air flow rate delivered from the air solar collector with a temperature and a humidity, respectively, 90 °C and 20 g water/kg dry air (point 2) undergo a humidification by adiabatic injection of water to increase its humidity approximately to 43 g water/kg dry air (point 3). In this case, the amount of water that can be gained is 23 g water/kg dry air.

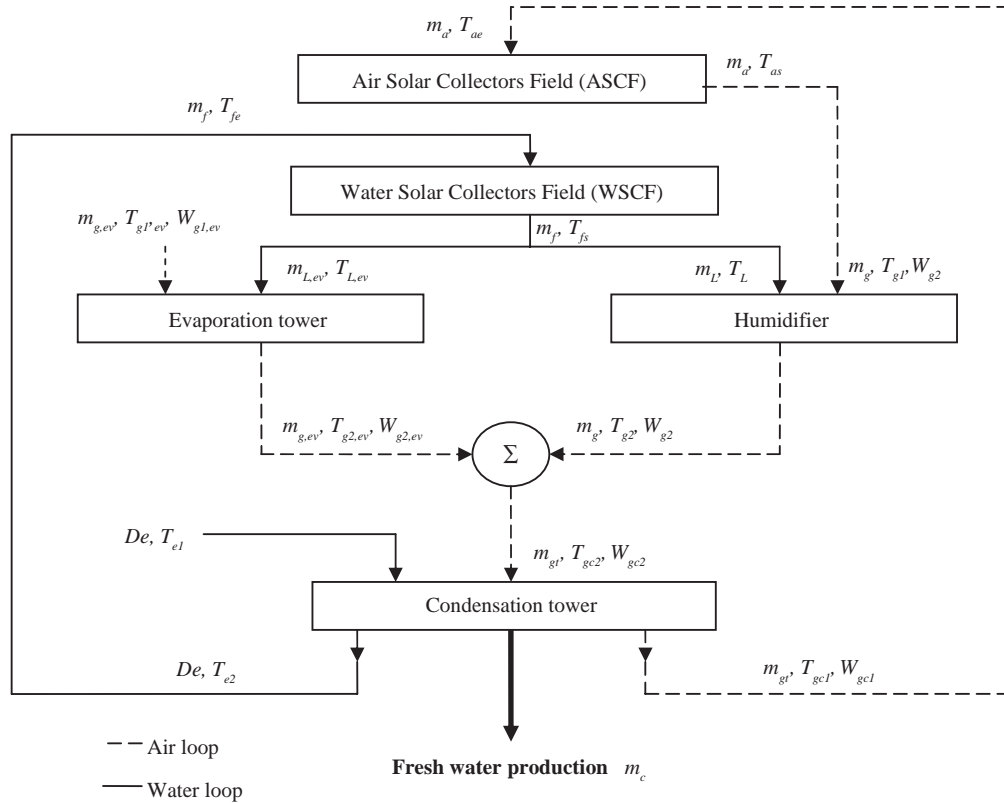


Fig. 3. A synoptic diagram of the entire process.

3. Global mathematical model

In a previous work [6], we have presented a detailed parametric study of the five components of the humidification – dehumidification solar desalination unit in steady state regime. Moreover, since these components are coupled and the output of each component is the input of the next, it is necessary to couple the various components of the present desalination unit and get a global steady state mathematical model that would provide a good description of the entire system. Fig. 3 presents a synoptic diagram of the entire process.

The steady state model of the entire desalination unit is obtained by coupling the individual models developed for the water solar collector, air solar collector, humidifier, evaporation tower and condensation tower. The obtained model is a set of equations. The model is based on some previous assumptions [6]. The following equations present the corresponding model.

- For the water solar collector

The energy balance equation for the system formed by the absorber and the fluid for a slice of the collector

with a width of l , a length of dx and a surface of ds , is the next one:

$$\frac{dT_f}{dx} = \frac{U_f l}{m_f C_f} \left(\frac{BI}{U_f} + T_{amb} - T_f \right) \quad (1)$$

- For the air solar collector

The thermal balances of the system formed by the absorber, air and the glass cover for a slice of the collector surface are the followings:

At the absorber plate

$$I \tau_v \alpha_{pl} = h_{radpl-v} (T_{pl} - T_v) + U_{loss} (T_{pl} - T_{amb}) + h_{conpl-a} (T_{pl} - T_a) \quad (2)$$

At the flowing air

$$\frac{dT_a}{dx} = \beta_1 (T_{pl} - T_a) + \beta_2 (T_v - T_a) \quad (3)$$

At the glass cover

$$I\alpha_v = h_{radv-pl}(T_v - T_{pl}) + h_{conv-a}(T_v - T_a) + h_{v-amb}(T_v - T_{amb}) \quad (4)$$

With: $h_{v-amb} = h_{conv-amb} + h_{radv-amb}$; overall heat transfer coefficient toward outside

- For the humidifier
 - Thermal balances

At the air phase

$$\frac{dT_g}{dx} = \frac{h_g a_h (T_g - T_i)}{m_g C_g} \quad (5)$$

At the water phase

$$\frac{dT_L}{dx} = \frac{h_L a_h (T_i - T_L)}{m_L C_L} \quad (6)$$

- Mass balances

At the air–water phase

$$\frac{dW_g}{dx} = \frac{K_m a_h (W_i - W_g)}{m_g} \quad (7)$$

- Enthalpy balances

$$m_L C_L dT_L = m_g C_g dT_g + m_g \lambda_o dW_g \quad (8)$$

To be numerically integrated, the above equations are completed with both empirical correlations of the voluminal heat coefficients ($h_L a_h, h_g a_h$) and mass transfer coefficient ($K_m a_h$) which are obtained by Ben Amara et al. [7] and an algebraic equation of water steam saturation curve [8].

$$h_L a_h = 25223 m_L^{0.0591} m_g^{0.1644} Z^{-0.0542}$$

$$K_m a_h = 0.6119 m_L^{0.1002} m_g^{0.3753} Z^{-0.0986}$$

The air-film voluminal heat transfer coefficient and the voluminal mass transfer on the air–water interface are related by Lewis relation [9] as follows:

$$h_g a_h = C_g K_m a_h$$

The curve of saturation of water steam is given by the following equation:

$$W_i = 0.62198 \frac{P_i}{1 - P_i} \quad (9)$$

- For the evaporation tower
 - At the air phase

$$\frac{dT_{g,ev}}{dz} = \frac{h_g a_{ev} (T_{i,ev} - T_{g,ev})}{m_{g,ev} C_{g,ev}} \quad (10)$$

- At the water phase

$$\frac{dT_{L,ev}}{dz} = \frac{h_L a_{ev} (T_{L,ev} - T_{i,ev})}{m_{L,ev} C_L} \quad (11)$$

- At the interface air–water

The mass balance equation at the interface level is given by the following one:

$$\frac{dW_{g,ev}}{dz} = \frac{K_m a_{ev} (W_{i,ev} - W_{g,ev})}{m_{g,ev}} \quad (12)$$

The thermal balance equation can be written under the following form:

$$h_L a_{ev} (T_{L,ev} - T_{i,ev}) = h_g a_{ev} (T_{i,ev} - T_{g,ev}) + \lambda_o K_m a_{ev} (W_{i,ev} - W_{g,ev}) \quad (13)$$

Like the mathematical model of the humidifier, to solve the above system of equations, it is necessary to complete these equations with empirical correlations of the voluminal heat coefficients ($h_L a_{ev}, h_g a_{ev}$) and mass transfer coefficient ($K_m a_{ev}$) which are developed by Ben Bacha et al. [2] and an algebraic equation of the curve of saturation of water steam [8].

$$h_L a_{ev} = 5900 m_{L,ev}^{0.169} m_{g,ev}^{0.5894}$$

$$K_m a_{ev} = 2.09 m_{L,ev}^{0.45} m_{g,ev}^{0.11515}$$

The voluminal mass transfer coefficient for air–water mixture is determined beforehand by Lewis relation:

$$h_g a_{ev} = C_{g,ev} K_m a_{ev}$$

The curve of saturation of water steam is given by the following equation:

$$W_{i,ev} = 0.62198 \frac{P_{i,ev}}{1 - P_{i,ev}} \quad (14)$$

• For the condensation tower

– At the water phase

$$\frac{dT_e}{dz} = \frac{UA(T_{ic} - T_e)}{D_e C_e} \quad (15)$$

– At the air phase

$$\frac{dT_{gc}}{dz} = \frac{h_{gc}A(T_{gc} - T_{ic})}{m_{gt}C_{gc}} + \frac{\lambda_o K_{mc}A(W_{gc} - W_{ic})}{m_{gt}C_{gc}} \quad (16)$$

– At the interface air-condensate

The mass balance equation at the interface air-condensate level is given by the following equation:

$$\frac{dW_{gc}}{dz} = \frac{K_{mc}A(W_{ic} - W_{gc})}{m_{gt}} \quad (17)$$

The thermal balance equation at the interface air-condensate can be written as follows:

$$W_{ic} = W_{gc} + \frac{h_{gc}(T_{gc} - T_{ic}) + U(T_e - T_{ic})}{\lambda_o K_{mc}} \quad (18)$$

The water condensation rate is determined by using an algebraic equation that relates the variation of the water content with the height of the tower:

$$dm_c = K_{mc}A(W_{ic} - W_{gc})dz \quad (19)$$

The saturation absolute humidity is given by the following equation:

$$W_{ic} = 0.62198 \frac{P_{ic}}{1 - P_{ic}} \quad (20)$$

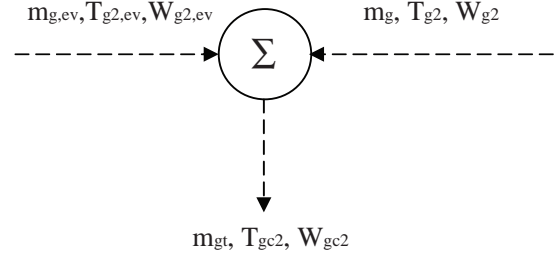
The calculation equations of all coefficients used in this paper are presented later in Appendix.

4. Boundary conditions

The outlet parameters of each component constituting the desalination unit are the input parameters for the next. So, it's necessary to introduce into the numerical computer package which is developed in order to

simulate the entire system, the following equations of coupling parameters at the entrance of each component:

– At the entrance of the condensation tower



$$W_{gc2} = \frac{m_g W_{g2} + m_{g,ev} W_{g2,ev}}{m_{gt}}$$

$$T_{gc2} = 87.2302 + 10.842 \text{Log}(W_{gc2}) - 2.6414 \text{Log}^2(W_{gc2}) - 0.3393 \text{Log}^3(W_{gc2})$$

$$D_e = N_f m_f$$

$$m_{gt} = m_g + m_{g,ev}$$

– At the entrance of the humidifier

$$m_g = N_a m_a; m_L = \frac{N_f m_f}{2}; T_{g1} = T_{as}; T_L = T_{fs}$$

– At the entrance of the evaporation tower

$$m_{L,ev} = \frac{N_f m_f}{2}; T_{L,ev} = T_{fs}$$

– At the entrance of the air solar collector

$$T_{ae} = T_{gc1}$$

– At the entrance of the water solar collector

$$T_{fe} = T_{e2}$$

5. Simulation and results discussion

The below simulation results were obtained for the properties of the entire desalination unit which are shown in Table 1.

In order to optimize the functioning of the developed unit according to the season of the year and climatic conditions, three operating modes have been

Table 1
Properties of the entire desalination unit used in simulation

Components	Description	Value/Type
ASCF	Aperture area	16 m ²
	Absorber plate material	Copper
	Absorptivity of plate	0.9
	Absorptivity of glass cover	0.1
	Back insulation, thickness	Polyurethane, 20 mm
	Emissivity of plate	0.94
	Emissivity of glass cover	0.987
	Transmissivity of glass cover	0.875
WSCF	Aperture area	7.2 m ²
	Effective transmission absorption	0.7
	Riser tubes material	Copper
	Absorber surface	Paint mat black
	Loss coefficient	4.8 W/m ² .K
	Back insulation, thickness	Fibre glass, 50 mm
Humidifier	Size	0.5 × 0.5 × 0.7 m ³
	Packed bed	Cellulosic materiel
Evaporation tower	Size	0.5 × 0.5 × 1.5 m ³
	Packed bed	Thorn tree
Condensation tower	Size	0.5 × 0.5 × 1.5 m ³

developed, based on the flexibility of the unit. These operating modes are: operating mode 1 using water solar collector, evaporation tower, condensation tower (Fig. 4); operating mode 2 using air solar collector, humidifier, evaporation tower and condensation tower (Fig. 5); operating mode 3 using water solar collector, air solar collector, humidifier, evaporation tower and condensation tower (Fig. 6).

Seen that the thermal capacity of air is low, the air solar collector is very sensible to the fluctuations of the solar radiation notably during both the winter and the night. Thus, a condensation of moist air can take place in the channels of the air solar collector. In this case, operating mode 1 was proposed.

During the summer and during the sunny days (high solar radiation), one can mingle the two circuits, that is to heat water and air. In this case, operating modes 1, 2 and 3 were proposed. The effect of the operating modes on the system productivity is illustrated by Fig. 7.

The productivity of the system is increased by 66% for the second operating mode (using air solar collector, humidifier, evaporation tower and condensation tower) compared to the first operating mode (using water solar collector, evaporation tower, condensation tower). Also, the system productivity is increased by 26% for the third operating mode (using water solar collector, air solar collector, humidifier, evaporation tower and condensation tower) compared to the second operating mode. Therefore, the third operating

mode proved to be the most effective one and is considered in this work.

The following simulation results display the influence of various operating and meteorological parameters on the fresh water production (m_c).

Fig. 8 illustrates the effect of the ratio of air flow rate to water flow rate in the humidifier on water condensation rate. It is noticeable that for each water flow rate corresponds an optimum air flow one for which the

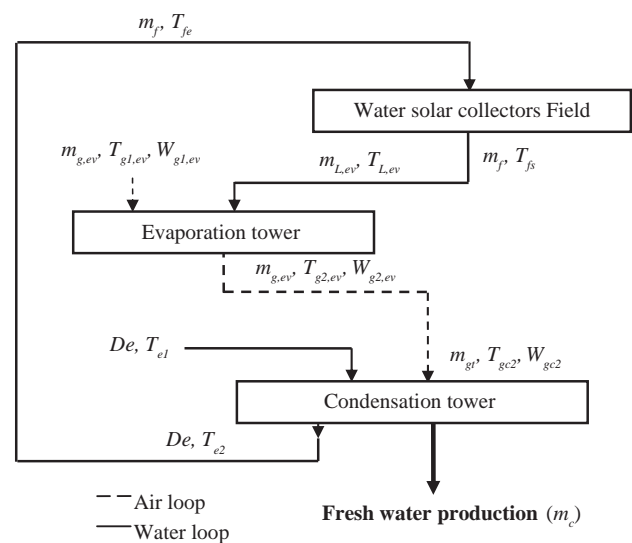


Fig. 4. Operating mode 1.

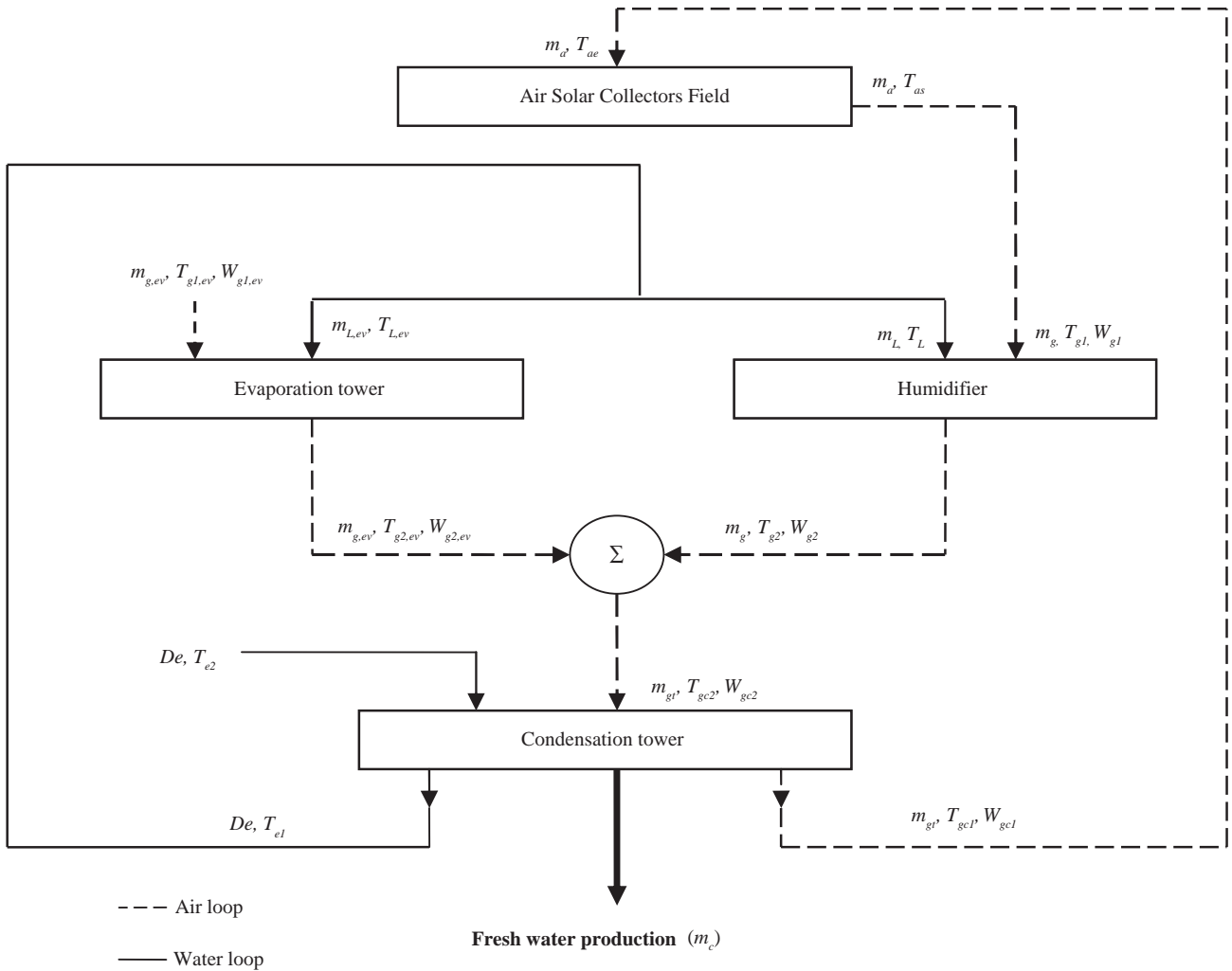


Fig. 5. Operating mode 2.

water condensation rate is maximum. We can also notice that this maximum increases with decreasing the water flow rate. This result can be explained by the fact that while decreasing the water flow rate, the temperature of the exiting water of solar water collector to the entrance of the evaporation tower and the humidifier, increases which in its part augments the rate of vaporization of water and, hence, the fresh water production.

Fig. 9 shows the influence of the temperature of air and water at the inlet of humidifier on the water condensation rate. It is clear that the temperature of water at the entrance of humidifier has more impact on water condensation rate than the temperature of air at the inlet of humidifier. This result is expected, because the heat capacity of water is roughly four times the heat capacity of air.

Figs. 10 and 11 show simulation results respectively for the effect of solar radiation and the effect of solar collector area on fresh water production. Fig. 10

displays that the production of the unit increases linearly according to the solar radiation. Indeed, the increase of the insolation increases the total energy won by the unit that increases the temperatures of both the water and air inlet to the tower of evaporation and to the humidifier. This provokes the increasing of water vaporization rate and then the fresh water production. From Fig. 11, one witnesses that the water solar collector surface influences more the production of the unit than the air solar collector surface. The principal reason explaining this result is that the air solar collector is only used to heat air at the entrance of the humidifier but the water solar collector is used to heat water at the entrance of the evaporation tower and the humidifier. Besides, the water solar collector is more efficient than the air solar collector [10]. This numerical result is in agreement with Nafey's [11].

Fig. 12 presents a comparison between present work and Ben Bacha's without taking account of the

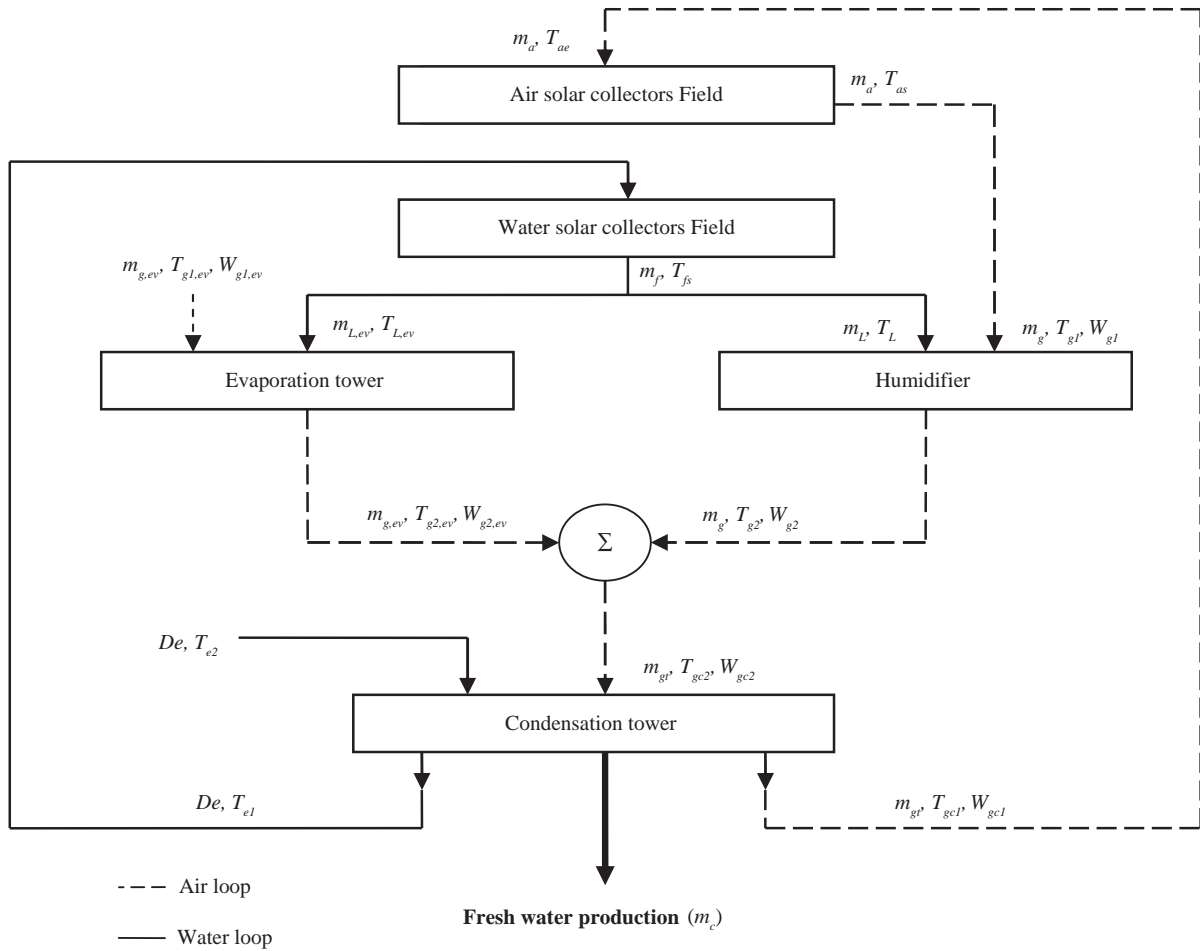


Fig. 6. Operating mode 3.

design’s properties of each component constituting the compared units. With reference to Fig. 10, it is clear that the production of fresh water of the present unit (water solar collector, air solar collector, evaporation tower,

humidifier and condensation tower) is increased by 59.5% for low values of water temperatures thereabouts 45 °C and by 28.5% for the high values of water

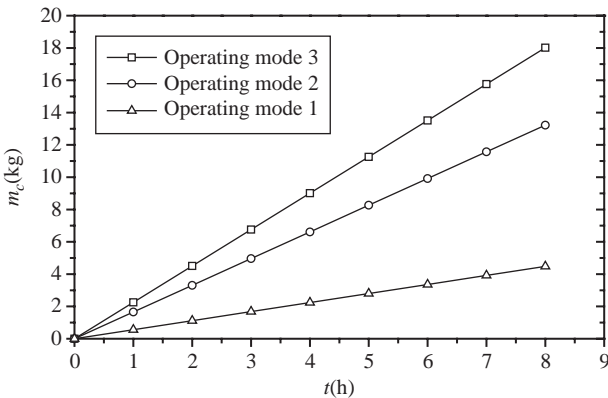


Fig. 7. The effect of the operating modes on the fresh water production $I = 900 \text{ W/m}^2$ and $T_{amb} = 30 \text{ }^\circ\text{C}$.

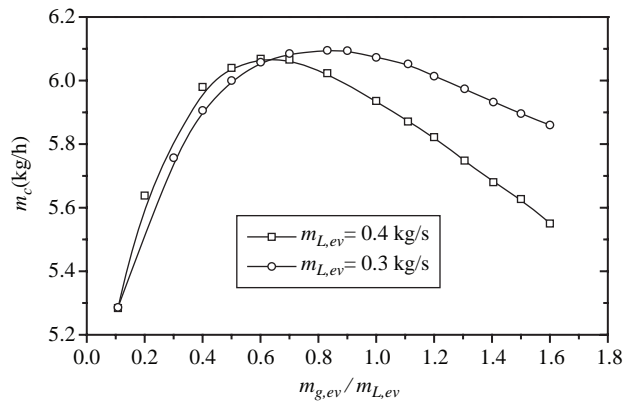


Fig. 8. Effect of the ratio $m_{g, ev} / m_{L, ev}$ on the fresh water production. $N_f = 6$, $N_a = 8$, $m_a = 0.06 \text{ kg/s}$, $m_f = 0.13 \text{ kg/s}$, $I = 800 \text{ W/m}^2$ and $T_{amb} = 25 \text{ }^\circ\text{C}$.

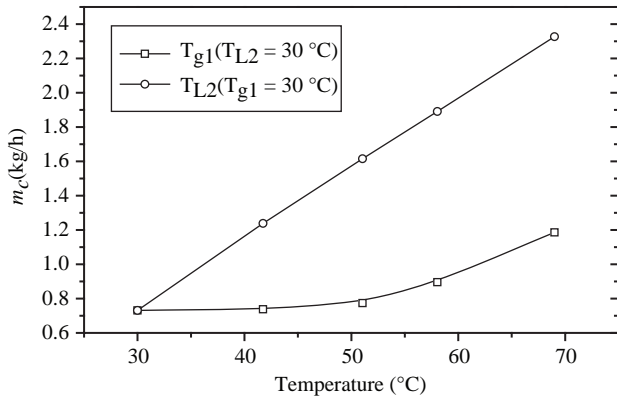


Fig. 9. Effect of the temperature of air and water at the inlet of the humidifier on the fresh water production. $N_f = 6$, $N_a = 8$, $m_a = 0.06$ kg/s, $m_f = 0.13$ kg/s, $m_{g,ev} = 0.48$ kg/s, $I = 800$ W/m² and $T_{amb} = 25$ °C.

temperatures thereabouts 70 °C by comparison to Ben Bacha’s unit [2] (water solar collector, evaporation tower and condensation tower).

6. Conclusion

A numerical computer program was developed using the Borland C++ software to solve the global mathematical model which was formulated based on heat and mass transfers. The developed mathematical model was simulated to investigate both the effect of different operating modes and that of the variation of functioning parameters and weather conditions on the fresh water production. It was found that the most effective operating mode consists of a flat plate solar air collector, a flat plate solar water collector, a humidifier, an evaporation tower and a condensation tower and the fresh water production of such unit has increased by

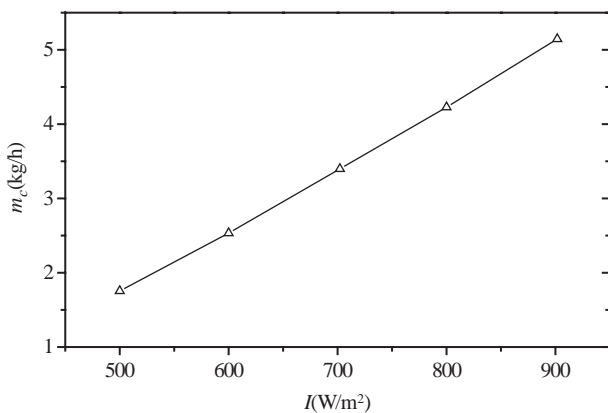


Fig. 10. Effect of solar radiation on the fresh water production $N_f = 6$, $N_a = 8$, $m_a = 0.06$ kg/s, $m_f = 0.13$ kg/s, $m_{g,ev} = 0.48$ kg/s and $T_{amb} = 25$ °C.

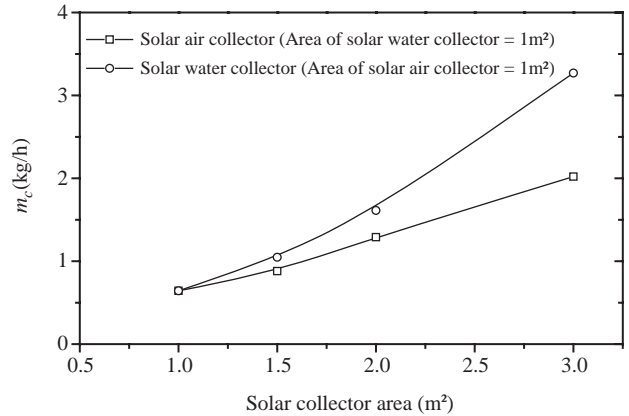


Fig. 11. Effect of solar collector area on fresh water production $m_a = 0.06$ kg/s, $m_f = 0.13$ kg/s, $m_{g,ev} = 0.48$ kg/s, $I = 800$ W/m² and $T_{amb} = 15$ °C.

59.5% for low values of water temperatures and by 28.5% for the high values of the latter by comparison with the SMCEC unit. The simulation results show also that:

For each water flow rate corresponds an optimum air flow rate for which the fresh water production is maximum.

The water temperature at the entrance of humidifier has more impact on the fresh water production than the air temperature at the inlet of humidifier.

The water solar collector surface influences more the fresh water production of the unit than the air solar collector surface.

The fresh water production is strongly affected by the solar radiation.

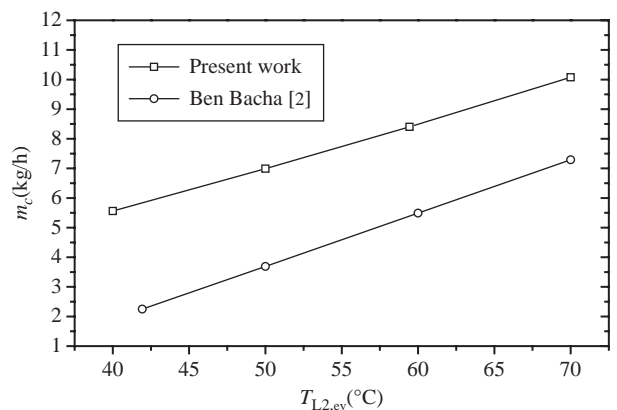


Fig. 12. Effect of inlet water temperature at the evaporation tower on fresh water production (comparison between present work and Ben Bacha et al. [2]). $N_f = 6$, $N_a = 8$, $m_a = 0.06$ kg/s, $m_f = 0.13$ kg/s, $m_{g,ev} = 0.48$ kg/s, $I = 800$ W/m² and $T_{amb} = 25$ °C.

Acknowledgements

The authors wish to express their heart-warming thanks and appreciation to the Ministère de l'Enseignement Supérieur, de la Recherche Scientifique et de la Technologie and to the Agence Nationale de la Maîtrise de l'Energie (ANME) for their financial support.

Special thanks are also dartsed to Mr R. Romdhani for his advice and help as far as English is concerned.

Symbols

A	air–water exchanger area in the condensation tower (m^2)	P_i	saturation pressure (Pa)
a	air–water exchanger area (m^2)	T	temperature (K)
B	effective transmission absorption product ($B = \tau\alpha$)	T_i	temperature at the air–water interface (K)
b	width of air solar collector	U	overall heat transfer coefficient in the condensation tower ($W/(m^2 K)$)
C_e	water specific heat ($J/(kg K)$)	U_f	overall energy loss from the absorber to outside ($W/(m^2 K)$)
C_f	fluid specific heat ($J/(kg K)$)	W	air humidity (kg water/kg dry air)
C_g	moist air specific heat in the humidifier ($J/(kg K)$)	W_i	saturation humidity (kg water/kg dry air)
C_{gc}	moist air specific heat in the condensation tower ($J/(kg K)$)	z_{ins}	insulation thickness of air solar collector (m)
$C_{g,ev}$	moist air specific heat in the evaporation tower ($J/(kg K)$)	Z	height of the humidifier packed bed (m)
D_e	water mass velocity in the condensation tower ($kg/(m^2 s)$)	z	coordinate in the flow direction (m)
D_{h1}	hydraulic diameter of air flow (m)	x	coordinate in the flow direction (m)
D_{h2}	hydraulic diameter of water flow (m)		
E	thickness of the condenser plate (m)		
g	gravitational acceleration (m/s^2)		
Gr	Grashof number		
H_g	enthalpy of air (J/kg)	<i>Greek</i>	
H_L	enthalpy of water (J/kg)	α	absorptance of the collector absorber surface
h	heat transfer coefficient ($J/(kg.K)$)	λ_o	latent heat of water evaporation (J/kg)
h_g	air heat transfer coefficient at the air–water interface ($W/(m^2.K)$)	λ_p	wall thermal conductivity ($W/m K$)
h_e	water heat transfer coefficient at the air–water interface ($W/(m^2.K)$)	λ_e	water thermal conductivity ($W/m K$)
l	width of water solar collector (m)	λ_c	condensed water thermal conductivity ($W/m K$)
L	length of air solar collector (m)	λ_{gc}	humid air thermal conductivity in the condensation tower ($W/m K$)
I	solar flux (W/m^2)	ρ_c	water density (kg/m^3)
K	thermal conductivity ($W/(m K)$)	μ_c	dynamic viscosity of condensed water (Ns/m^2)
K_m	water vapor mass transfer coefficient at the air–water interface ($kg/(m^2.s)$)	σ	Stefan-Boltzman constant
m	mass flow rate (kg/s)	ν	velocity of fluid (m/s)
m_c	fresh water production (kg/s)	τ	transmittance
m_{gt}	total mass velocity of moist air in the condenser ($kg/(m^2.s)$)		
Pr	Prandtl number	<i>Subscripts</i>	
Re	Reynolds number	1	tower bottom
N_f	number of water solar collector	2	tower top
N_a	number of air solar collector	a	air
		amb	ambient
		c	condensation tower
		con	convection
		e	cooling water
		v	glass cover
		ev	evaporation tower
		f	fluid
		g	moist air
		h	humidifier
		$loss$	loss to ambient
		pl	absorber plate
		rad	radiation

References

- [1] F. Ben Jemaa, I. Houcine and M.H. Chahbani, Potential of renewable energy development for water desalination in Tunisia, Renewable Energy J., 18 (1999) 331-347.

- [2] H. Ben Bacha., M. Bouzguenda, M.S Abid and A.Y. Maalej, Modeling and simulation of a water desalination station with solar multiple condensation evaporation cycle technique. *Renewable Energy*, 18 (1999) 349-365.
- [3] S. Parekh, M.M. Farid, J.R. Selman, and S. Al-Hallaj, Solar desalination with a humidification dehumidification technique a comprehensive technical review, *Desalination*, 160 (2004) 167-186.
- [4] W. Haeussler, *Das Mollier-i-x-Diagramm für feuchte Luft und seine technische Anwendungen*, Dresden und Leipzig, Steinkopf, 1960.
- [5] R. Mollier, Ein neues Diagramm für Dampf-Luft-Gemische, *Z.VDI* 67 (1923) and 73 (1929).
- [6] K. Zhani, H. Ben Bacha, T. Damak, *A study of a water desalination unit using solar energy*. *Int. J. Desalination Water Treatment*, in press.
- [7] M. Ben Amara, I. Houcine, A.A. Guizani and M. Mâalej, Theoretical and experimental study of a pad humidifier used on an operating seawater desalination process, *Desalination*, 168 (2004) 1-12.
- [8] ASHRAE, *Fundamental handbook Tome V-1977*.
- [9] M.A. Younis, M.A. Fahim, N. Wakao. Heat input-response in cooling tower-zeroth moments of temperature variations. *J. Chem. Eng. Jpn.*, 20 (1987) 614-618.
- [10] M. Laplante, *Étude numérique et expérimentale d'un distillateur d'eau salée à énergie solaire*, M.Sc. Thesis, Université de Sherbrooke, Canada, 2003.
- [11] A.S. Nafey, H.E.S. Fath, S.O. El-Helaby and A.M. Soliman, Solar desalination using humidification dehumidification processes. Part I. A numerical investigation, *Energy Conv. Mgmt.*, 45(7–8) (2004) 1243-1261.

Appendix

$$\beta_1 = \frac{bh_{conpl-a}}{m_a C_a}$$

$$\beta_2 = \frac{bh_{conv-a}}{m_a C_a}$$

$$h_{radpl-v} = \frac{\sigma(T_{pl}^2 + T_v^2)(T_{pl} + T_v)}{\frac{1}{\varepsilon_{pl}} + \left(\frac{1}{\varepsilon_v} - 1\right)}$$

$$h_{conpl-a} = 0.0336 \left(\frac{K_{pl}}{L}\right) \left(\frac{Lv_a}{\nu}\right)^{0.8}$$

$$h_{conv-a} = 0.0336 \left(\frac{K_v}{L}\right) \left(\frac{Lv_a}{\nu}\right)^{0.8}$$

$$h_{conpl-amb} = 5.7 + 3.8V_{wind}$$

$$h_{conv-amb} = 5.7 + 3.8V_{wind}$$

$$h_{radv-amb} = \varepsilon_v \sigma (T_v^2 + T_{amb}^2) (T_v + T_{amb})$$

$$U_{loss} = \frac{1}{\frac{1}{h_{conpl-amb}} + \frac{z_{ins}}{K_{ins}}}$$

$$U = \frac{1}{\frac{1}{h_c} + \frac{e}{\lambda_p} + \frac{1}{h_c}}$$

$$h_e = 0.023 \frac{\lambda_e}{D_{h2}} \text{Re}^{0.8} \text{Pr}^{0.33}$$

$$h_c = \sqrt[4]{\frac{\rho_c^2 g \lambda_o \lambda_c^3}{4\mu_{cz}(T_{ic} - T_p)}}$$

$$h_{gc} = 0.479 \frac{\lambda_{gc}}{D_{h1}} Gr^{1/4}$$

$$K_{mc} = \frac{h_{gc}}{C_{gc}}$$

$$\ln(P_i) = -6096.938 \frac{1}{T_i} + 21.240964 - 2.71119 \cdot 10^{-2} T_i + 1.67395 \cdot 10^{-5} T_i^2 + 2.43350 \ln(T_i)$$